

Full-Length Research Report

Longitudinal Changes in Individual *BrainAGE* in Healthy Aging, Mild Cognitive Impairment, and Alzheimer's Disease

Katja Franke¹, Christian Gaser^{1,2},
for the Alzheimer's Disease Neuroimaging Initiative

¹Structural Brain Mapping Group, Department of Psychiatry, Jena University Hospital, Jena, Germany

²Department of Neurology, Jena University Hospital, Jena, Germany

Abstract. We recently proposed a novel method that aggregates the multidimensional aging pattern across the brain to a single value. This method proved to provide stable and reliable estimates of brain aging – even across different scanners. While investigating longitudinal changes in *BrainAGE* in about 400 elderly subjects, we discovered that patients with Alzheimer's disease and subjects who had converted to AD within 3 years showed accelerated brain atrophy by +6 years at baseline. An additional increase in *BrainAGE* accumulated to a score of about +9 years during follow-up. Accelerated brain aging was related to prospective cognitive decline and disease severity. In conclusion, the *BrainAGE* framework indicates discrepancies in brain aging and could thus serve as an indicator for cognitive functioning in the future.

Keywords: *BrainAGE*, Alzheimer's disease, mild cognitive impairment, structural MRI, pattern recognition

Introduction

During normal brain development and aging, the brain is affected by progressive (e.g., cell growth and myelination) and by regressive (e.g., cell death and atrophy) neuronal processes (Silk & Wood, 2011). Those processes have been found to follow a specific pattern, with gray matter (GM) volume increasing in the first years of life and thereafter decreasing continuously; and with white matter (WM) volume increasing steadily until around the age of 20 when it plateaus (Good et al., 2001; Pfefferbaum et al., 1994). Healthy brain aging has been found to follow a specific heterogeneous and complex pattern of atrophy across the adult lifespan (Good et al., 2001), with normal age-related GM decline being inversely related to the phylogenetic origin of each respective region, i.e., younger structures being the last to mature as well as being more vulnerable to neurodegeneration (Terribilli et al., 2009; Toga, Thompson, & Sowell, 2006).

With the growing number of studies that have investigated both normal and abnormal age-related brain changes, most major neuropsychiatric disorders are now thought to arise due to deviations from normal brain development

(Gogtay & Thompson, 2010). Also diseases such as Alzheimer's disease (AD) and schizophrenia alter brain structures in diverse and abnormal modes (Ashburner et al., 2003; Meda et al., 2008). AD in particular is widely assumed to reflect accelerated aging (Cao, Chen-Plotkin, Plotkin, & Wang, 2010; Jones et al., 2011; Saetre, Jazin, & Emilsson, 2011), with accelerated age-related changes in brain atrophy being already evident at the stage of mild cognitive impairment (MCI), i.e., the prodromal stage of AD (Driscoll et al., 2009; Spulber et al., 2010). Additional evidence for this view was recently provided by showing that the atrophied regions detected in AD patients are largely overlapping with regions showing a normal age-related decline in age-matched healthy control subjects (Dukart, Schroeter, & Mueller, 2011).

Given the widespread but well-ordered brain tissue loss that occurs as a function of age-based processes, a straightforward and efficient solution might be to model healthy brain aging in order to subsequently identify abnormal aging processes and accelerated brain atrophy before the onset of upcoming clinical symptoms. Recently, we introduced a new approach based on structural magnet resonance imaging (MRI) data that enables to reliably estimate the brain age of

any given subject (Franke, Ziegler, Klöppel, Gaser, & Initiative, A. S. D. N., 2010). By employing kernel regression methods in a large training database, the complex, multidimensional aging patterns across the whole brain are detected and finally aggregated to a single value, i.e., the estimated brain age (Figure 1A). The individual discrepancies between estimated and chronological age were termed *brain-age gap estimation (BrainAGE)* score, with observed differences in *BrainAGE* scores being interpreted as originating from structural brain changes that show the pattern of accelerated (or decelerated) aging. Consequently, although only one MRI scan per subject is employed, the degree of acceleration or deceleration of brain aging can be quantified directly in terms of years, allowing a wide range of analyses and predictions on an individual level. For example, if a 70-year-old individual has a deviating *BrainAGE* score of +5 years, this means that this individual shows the typical atrophy pattern of a 75-year-old individual (Figure 1B). The framework comprises well-established and fully automatic processing steps of the MRI data, combines data from different scanners, and accurately estimates the age of healthy individuals with a correlation of $r = 0.92$ between estimated and chronological age. Furthermore, this brain-age estimation model has showed its potential to provide clinically relevant information by reporting a statistically significant, positive deviation of 10 years between estimated and chronological age in AD patients from the Alzheimer's Disease Neuroimaging Initiative (ADNI) database, indicating structural brain changes that show the pattern of accelerated aging (Franke et al., 2010). Additionally, a slightly modified *BrainAGE* approach recently provided a reliable reference curve based on structural MRI data, allowing for the prediction of structural brain maturation and a fast identification of developmental delays in childhood and adolescence (Franke, Luders, May, Wilke, & Gaser, 2012).

By implementing this new method of brain-age estimation, our present studies further analyze the stability and reliability of the *BrainAGE* approach, utilizing two subsamples that have (1) a short delay between two scans of the same subject on the same scanner (1.5T) as well as (2) two scans of the same subjects with two different field strengths (1.5T and 3.0T). Second, within a follow-up period of up to 4 years we explored the patterns of longitudinal changes in individual *BrainAGE* and quantified about 400 cognitively normal, MCI, and AD subjects. Further, we related discrepancies in brain aging to prospective cognitive functioning and disease severity.

Methods

ADNI Database

Part of the data used in the preparation of this article were obtained from the ADNI database (<http://adni.loni.ucla.edu>). The ADNI was launched in 2003 by the National Institute on Aging (NIA), the National Institute of Biomedical Imaging and Bioengineering (NIBIB), the Food and Drug Administration (FDA), private pharmaceutical companies, and non-profit organizations, as a \$60 million, 5-year public-private partnership. The primary goal of ADNI was to test whether serial MRI, positron emission tomography (PET), other biological markers as well as clinical and neuropsychological assessment can be combined to measure the progression of MCI and early AD. Determination of sensitive and specific markers of very early AD progression should aid researchers and clinicians in developing new treatments and monitoring their effectiveness as well as lessening the time and cost of clinical trials.

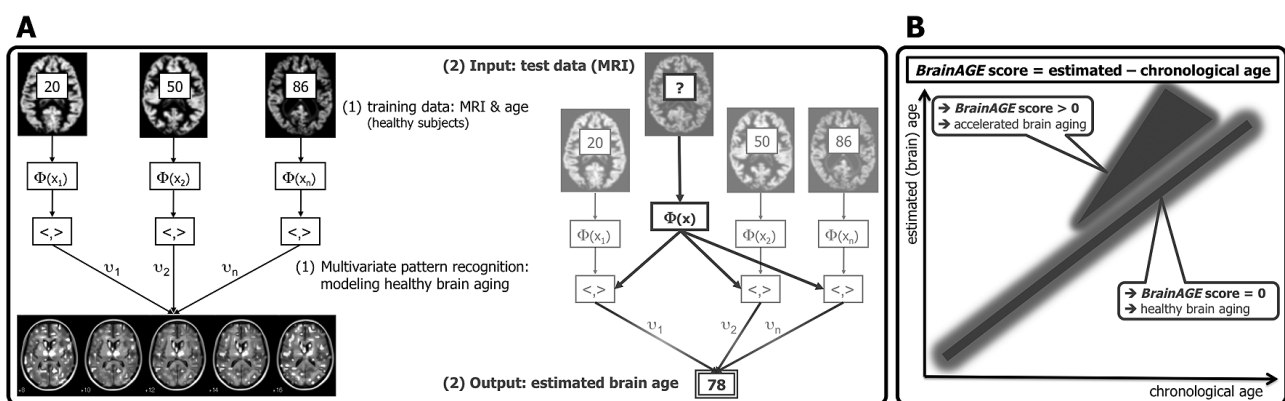


Figure 1. Depiction of the *BrainAGE* concept. (A) The model of healthy brain aging is trained with the chronological age and preprocessed structural MRI data of a training sample (left, with an exemplary illustration of the most important voxel locations that were used by the age regression model). Subsequently, the individual brain ages of previously unseen test subjects are estimated, based on their MRI data (blue, picture modified from Schölkopf et al., 2002[not in refs, or Schölkopf & Smola?]). (B) The difference between the estimated and chronological age results in the *BrainAGE* score. Consequently, positive *BrainAGE* scores indicate accelerated brain aging (blue area; for more detailed information please see Franke, Ziegler, Klöppel, Gaser, & Initiative, A. S. D. N., 2010).

The principal investigator of this initiative is Michael W. Weiner, MD, VA Medical Center and University of California – San Francisco. ADNI is the result of efforts of many coinvestigators from a broad range of academic institutions and private corporations, and subjects have been recruited from over 50 sites across the United States and Canada. The initial goal of ADNI was to recruit 800 adults, aged 55 to 90, to participate in the research; approximately 200 cognitively normal older individuals to be followed for 3 years; 400 people with MCI to be followed for 3 years; and 200 people with early AD to be followed for 2 years. For up-to-date information, see <http://www.adni-info.org>.

Subjects

To train the age estimation framework, we used T₁-weighted MRI data of 560 healthy subjects (249 males) from the publicly accessible IXI cohort (<http://www.brain-development.org>; data downloaded in September 2011) aged 20–86 years, which were collected on three different scanners (Philips 1.5T, General Electric 1.5T, Philips 3.0T).

Before analyzing the individual patterns of longitudinal *BrainAGE* changes, the stability of *BrainAGE* estimations within the same subjects were explored using two different subsamples. The first test sample included structural MRI data of 20 healthy subjects (aged 19–34 years) from the Open Access Series of Imaging Studies database (OASIS; Marcus et al., 2007; <http://www.oasis-brains.org>), for whom a short-delay (less than 90 days) double scan on the same scanner was available (Siemens 1.5T). The second test sample included 1.5T as well as 3.0T structural MRI data (acquired within a short delay) of 60 healthy nondemented elderly subjects (aged 60–87 years) from the ADNI database (data downloaded in May 2010). The characteristics of all three samples are given in Table 1.

To investigate the longitudinal pattern of *BrainAGE*

Table 1. Characteristics of the subjects in the training group (IXI) and both test samples (OASIS and ADNI) double-scanned within a short delay (< 90 days)

	Training sample Test samples		
	IXI	OASIS	ADNI
No. subjects	560	20	60
Males/Females	249/311	8/12	22/38
Age mean (<i>SD</i>)	48.6 (16.5)	23.4 (4.0)	75.2 (4.8)
Age range	20–86	19–34	60–87
No. of MRI scanners (1.5T/3T)	2/1	1/0	26/26

Notes. Please explain use of *italics!*

changes in healthy aging, MCI, and AD, a third test sample included all subjects from the ADNI database for whom at least the baseline scan and one follow-up scan were available (1.5T). Adopting the diagnostic classification at baseline and follow-up, subjects were grouped as (1) NO (healthy subjects) if diagnosis was NO at baseline and 3-year follow-up [$n = 108$]; (2) sMCI (stable MCI) if diagnosis was MCI at baseline and 3-year follow-up [$n = 36$]; (3) pMCI (progressive MCI) if diagnosis was MCI at baseline and AD at some follow-up, without reversion to MCI or NO [$n = 112$]; (4) AD patients if diagnosis was AD at baseline, without reversion [$n = 150$]. For further analyses we used baseline and follow-up test scores of the cognitive scales: Alzheimer's Disease Assessment Scale (ADAS; Mohs, 1996; Mohs & Cohen, 1988; range 0–85, with higher test scores being related to worse cognitive functioning), global Clinical Dementia Rating Scale (CDR; Morris, 1993; range 0–3, with 0 denoting cognitively healthy, 0.5 denoting mild cognitive impairments, and a score of 1 or above denoting AD), and Mini-Mental State Examination (MMSE; Cockrell & Folstein, 1988; range 0–30, with lower scores being related to higher disease severity). The baseline and follow-up characteristics of this test sample are given in Table 2.

Table 2. Characteristics of the ADNI test sample for longitudinal analyses

		NO	sMCI	pMCI	AD
Baseline	No. subjects	108	36	112	150
	Males/females	61/47	30/6	67/45	76/74
	Age mean (<i>SD</i>)	75.6 (5.0)	77.0 (6.1)	74.5 (7.4)	74.6 (7.6)
	MMSE mean (<i>SD</i>)	29.22 (0.89)	27.42 (1.87)	26.62 (1.75)	23.45 (1.95)
	CDR mean (<i>SD</i>)	0.00 (0.00)	0.50 (0.00)	0.50 (0.00)	0.73 (0.25)
Follow-up	ADAS mean (<i>SD</i>)	8.84 (3.84)	17.29 (5.88)	21.77 (5.70)	28.78 (7.85)
	No. scans (<i>SD</i>)	5.02 (0.77)	5.86 (0.87)	5.20 (1.38)	3.45 (0.74)
	Follow-up duration in days (<i>SD</i>)	1194 (261)	1114 (244)	969 (360)	609 (222)
	Age at last scan (<i>SD</i>)	78.9 (5.0)	80.1 (6.0)	77.2 (7.6)	76.3 (7.7)
	MMSE at last scan (<i>SD</i>)	29.01 (1.27)	27.11 (2.63)	21.62 (4.28)	19.28 (5.64)
	CDR at last scan (<i>SD</i>)	0.06 (0.16)	0.49 (0.15)	0.92 (0.42)	1.27 (0.67)
	ADAS at last scan (<i>SD</i>)	10.11 (5.44)	17.64 (6.48)	32.53 (9.48)	38.14 (12.14)

Notes. Abbreviations: AD, Alzheimer's disease; ADAS, Alzheimer's Disease Assessment Scale; CDR, clinical dementia rate; MMSE, Mini-Mental State Examination; NO, healthy control subjects; pMCI, progressive mild cognitive impairment; *SD*, standard deviation; sMCI, stable mild cognitive impairment.

Preprocessing of MRI Data and Data Reduction

Preprocessing of the T1-weighted images was done using the SPM8 package (<http://www.fil.ion.ucl.ac.uk/spm>) and the VBM8 toolbox (<http://dbm.neuro.uni-jena.de>), running under MATLAB. All T1-weighted images were corrected for bias-field inhomogeneities, then spatially normalized and segmented into GM, WM, and cerebrospinal fluid (CSF) within the same generative model (Ashburner & Friston, 2005). The segmentation procedure was further extended by accounting for partial volume effects (Tohka, Zijdenbos, & Evans, 2004), by applying adaptive maximum a posteriori estimations (Rajapakse, Giedd, & Rapoport, 1997), and by using a hidden Markov random field model (Cuadra, Cammoun, Butz, Cuisenaire, & Thiran, 2005) as described previously (Gaser, 2009). The images were processed with affine registration and smoothed with 4-mm full-width-at-half-maximum smoothing kernels.

BrainAGE Framework

The *BrainAGE* framework utilizes a high-dimensional pattern recognition method, i.e., relevance vector regression (RVR; Tipping, 2001), to model healthy brain aging. RVR was introduced by Tipping (2000) as a Bayesian alternative to support vector machines (SVM), but is easier to use since all model parameters are automatically estimated by the learning procedure itself. More details can be found in Bishop (2006), Schölkopf and Smola (2002), and Tipping (2000). Recently, the *BrainAGE* framework proved to be a reliable, scanner-independent, and efficient method for age estimation in healthy subjects (Franke et al., 2010). It resulted in a correlation of $r = 0.92$ between the estimated and the real age in the test samples, and a mean absolute error of 5 years. Furthermore, the study identified the number of training samples as the critical factor for prediction accuracy.

In general, the age regression model is trained with the chronological age and preprocessed whole brain structural MRI data of the training sample, resulting in a complex model of healthy brain aging (Figure 1A, left). Subsequently, the brain age of a test subject can be estimated using the individual tissue-classified MRI data, aggregating the complex, multidimensional aging pattern across the whole brain into one single value (Figure 1A, right). The difference between estimated and chronological age results in the *BrainAGE* score, which consequently directly quantifies the amount of acceleration or deceleration in brain aging (Figure 1B). For training the model as well as for predicting individual brain ages, we used "The Spider" (<http://www.kyb.mpg.de/bs/people/spider/main.html>), a freely available toolbox running under MATLAB. For more detailed information please refer to Franke et al. (2010).

Within this study, the linear combination of whole brain GM and WM images were used to train the *BrainAGE* framework. Data reduction was performed by applying principal component analysis (PCA), utilizing the "Matlab Toolbox for Dimensionality Reduction" (<http://ict.ewi.tudelft.nl/~lvan-dermaaten/Home.html>). PCA was performed only on the training sample. The estimated transformation parameters were subsequently applied to the test samples, allowing estimation of individual brain ages based on baseline MRI data. The difference between the estimated and the chronological age resulted in the *BrainAGE* score, indicating accelerated (positive values) or decelerated (negative values) brain aging.

Statistical Analysis

In the first analysis, the intraclass correlation coefficient (ICC; two-way random single measures) as well as Student's *t*-test was calculated for each test sample separately to assess the conformity and stability of *BrainAGE* estimations across several MRI scans within a short delay (OASIS) and across different scanner field-strengths (ADNI).

In the second analysis, the longitudinal changes in individual *BrainAGE* scores, which were corrected for age and gender, were fitted against days from baseline with a multivariate linear regression model. Baseline *BrainAGE* scores, *BrainAGE* scores at last visit, and longitudinal changes in *BrainAGE* were compared among the four diagnostic groups using an analysis of variance (ANOVA). Posthoc analyses (with Bonferroni adjustment to compensate for multiple comparisons) were conducted to further explore significant group differences. The relationship between *BrainAGE* scores and cognitive scales (i.e., MMSE, CDR, ADAS) were explored using Pearson's linear correlation coefficients. ICC was calculated using SPSS. All other statistical testing was performed using MATLAB.

Results

Stability of *BrainAGE* Estimations

The *BrainAGE* estimations within the same subjects proved to be stable across a short delay between two scans as well as across scanners. In the OASIS subsample, in which the subjects had a short delay between two scans on the same scanner (1.5T), the brain-age estimations resulted in mean (*SD*) raw *BrainAGE* scores of 13.8 (6.1) years for the 1st and 12.8 (5.6) years for the 2nd scan (Figure 2A). The raw *BrainAGE* scores derived from the 1st as well as 2nd scan significantly differed from a zero mean ($p < .001$), but not among each other ($p = .60$). The correlation between the raw *BrainAGE* scores derived from the 1st and 2nd scan data resulted in $r = 0.93$ ($p < .001$). Thus, the results suggest a systematical data-specific offset at each of both scanning time points. For illustration reasons and/or

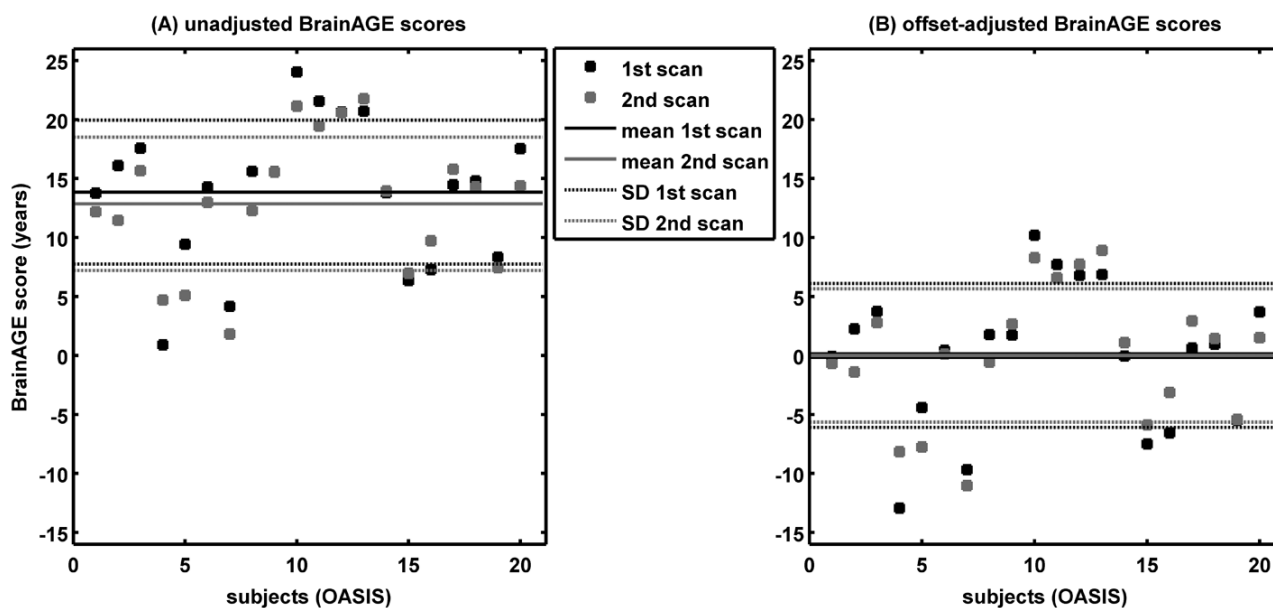


Figure 2. Unadjusted (A) and offset-adjusted (B) *BrainAGE* scores for double-scanned OASIS subjects on the same scanner within a short delay. ICC between the *BrainAGE* scores calculated from the 1st and 2nd scan was 0.93.

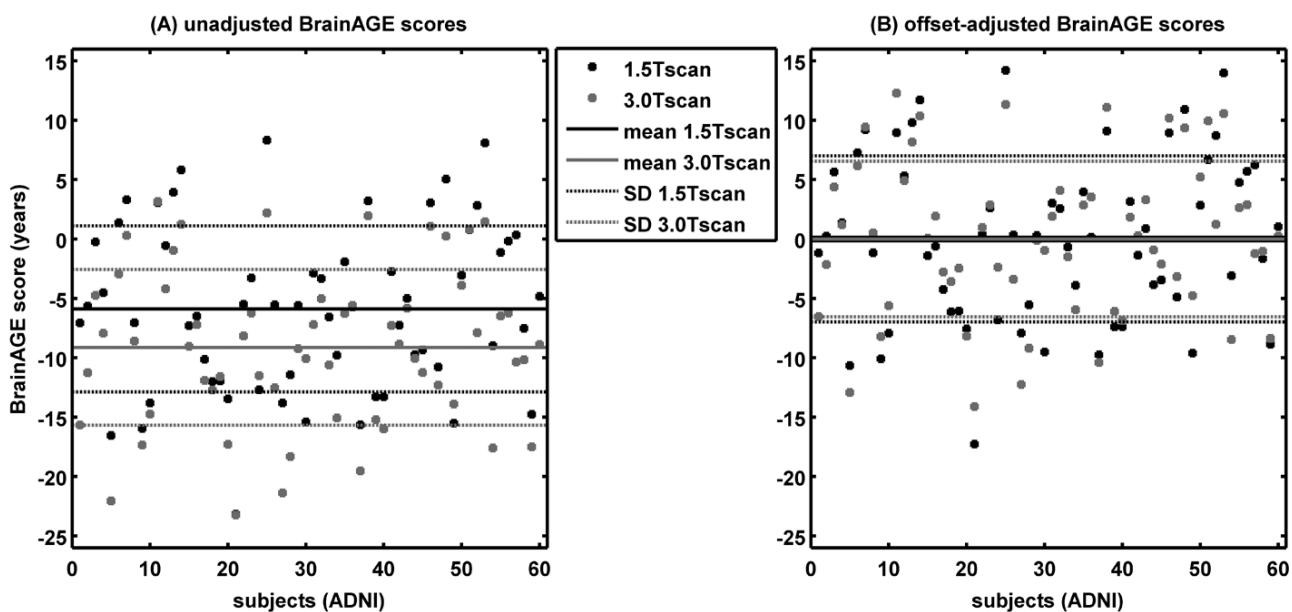


Figure 3. Unadjusted (A) and offset-adjusted (B) *BrainAGE* scores for double-scanned ADNI subjects on 1.5T and 3.0T scanner within a short delay. ICC between the *BrainAGE* scores calculated from the 1.5T and 3.0T scan was 0.90.

better interpretability of the results, this offset can be easily adjusted by a linear shift, i.e., setting the *BrainAGE* scores to a zero group mean (Figure 2B). Linearly adjusting for the offset at each scanning time point separately, resulted in a correlation between raw and adjusted *BrainAGE* scores of $r = 0.996$ ($p < .001$). The ICC between the *BrainAGE* scores calculated from the 1st and 2nd scan was 0.93 [95% confidence interval (CI): 0.83–0.97], demonstrating strong stability of the estimated *BrainAGE* scores across several MRI scans.

The ADNI subsample, which included only nondemented subjects who had two baseline scans from MRI scanners of two different field strengths (1.5T and 3.0T) showed mean (*SD*) raw *BrainAGE* scores of -5.9 (7.0) years for the 1.5T data and -9.1 (6.6) years for the 3.0T data (Figure 3A), with a correlation between both scans of $r = 0.91$ ($p < .001$). The raw *BrainAGE* scores derived from the 1.5T as well as 3.0T data significantly differed from a zero mean ($p < .001$). These results additionally suggest a strong dependency of brain-age estimation on field strength, with

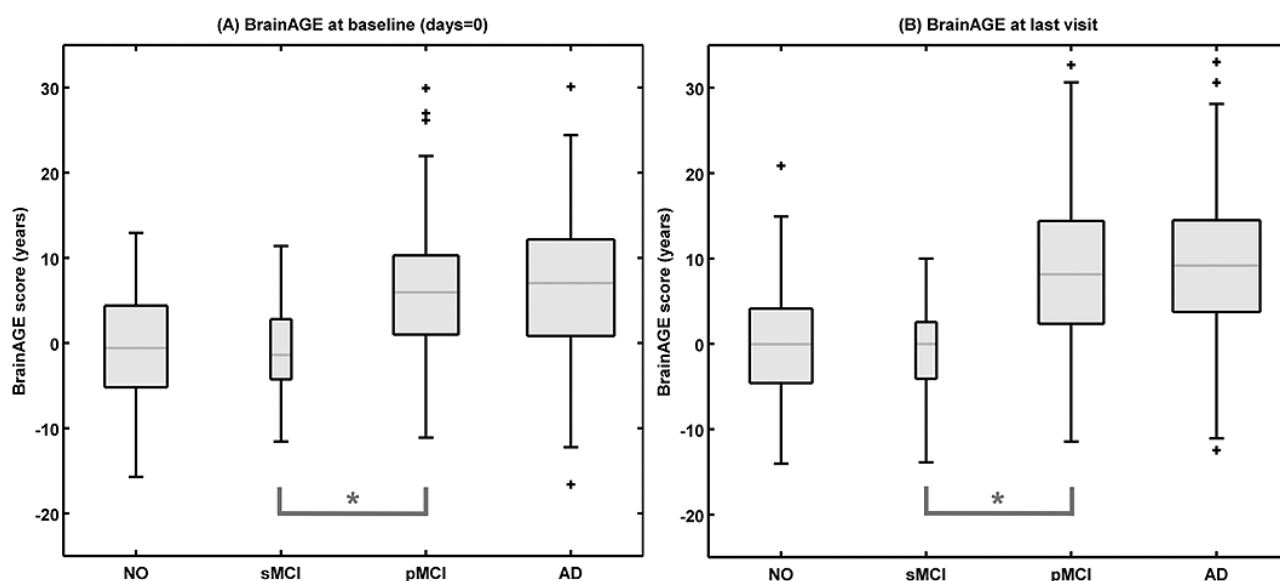


Figure 4. Box plots of (A) baseline *BrainAGE* scores and (B) *BrainAGE* scores of last MRI scans for all diagnostic groups. Posthoc *t*-tests showed significant differences between NO/sMCI vs. pMCI/AD ($p < .05$; red lines) at both time measurements. The gray boxes contain the values between the 25th and 75th percentiles of the samples, including the median (dashed line). Lines extending above and below each box symbolize data within 1.5 times the interquartile range (outliers are displayed with a “+”). The width of the boxes depends on the sample size.

1.5T MRI data resulting in larger *BrainAGE* scores than those derived with 3.0T MRI data. Again, this offset can be easily adjusted by a linear shift as described above (Figure 3B). After linearly adjusting for the field strength-specific offset, Student’s *t*-test resulted in no difference between the *BrainAGE* scores calculated from the 1.5T and 3.0T scan ($p = 1.00$). ICC between the *BrainAGE* scores calculated from the 1.5T and 3.0T scan was 0.90 [CI: 0.84–0.94], demonstrating strong stability of the estimated *BrainAGE* scores across different field strengths. Taken together, these results suggest that the *BrainAGE* framework reliably estimates individual brain age based on structural MRI data.

Longitudinal *BrainAGE* Estimation

In the longitudinal ADNI sample, the baseline *BrainAGE* scores differed among the four groups ($F = 26.8$; $p < .001$). For better interpretability, all individual *BrainAGE* scores were adjusted by a linear shift determined in the NO group (as described in “Stability of *BrainAGE* estimations”). Thus, the baseline *BrainAGE* scores resulted in the following group means: NO = -0.30 years, sMCI = -0.48 years, pMCI = 6.19 years, and AD = 6.67 years (Figure 4A). Posthoc *t*-tests showed significant differences between NO/sMCI vs. pMCI/AD ($p < .05$), suggesting structural brain changes that show the pattern of accelerated aging in the pMCI and AD groups. Regarding NO and sMCI subjects, the estimated brain age at baseline did not differ sig-

nificantly from the chronological age ($p = .61$ in both groups).

The *BrainAGE* scores remained stable for the NO and the sMCI groups across the follow-up period of up to 4 years, but increased in the pMCI and AD groups, suggesting additional acceleration in brain aging in the pMCI and AD groups. The fit of the longitudinal changes in *BrainAGE* resulted in the following changing rates (*BrainAGE* years per follow-up year): NO = 0.12, sMCI = 0.07, pMCI = 1.05, and AD = 1.51 (Figure 5). These rates differed among the groups ($F = 23.1$; $p < .001$), with posthoc *t*-tests showing significant differences between NO/sMCI vs. pMCI/AD ($p < .05$). At the last MRI scan of each subject, the *BrainAGE* scores also differed among the groups ($F = 44.0$; $p < .001$), resulting in the following: NO = -0.06 years, sMCI = -0.38 years, pMCI = 8.96 years, and AD = 9.02 years (Figure 4B). Again, posthoc *t*-tests showed significant differences between NO/sMCI vs. pMCI/AD ($p < .05$). Regarding NO and sMCI subjects, the estimated brain age at baseline did not differ significantly from the chronological age ($p = .92$ and $p = .68$, respectively).

Taken together, these results suggest that the acceleration in brain aging in pMCI and AD found at baseline becomes even more accelerated during the next months and years. On the other hand, the results suggest that brain aging in NO and sMCI remained stable during the follow-up period of 4 years, showing only normal age-related atrophy.

Across the whole sample, the *BrainAGE* scores at baseline were moderately correlated with cognitive functioning and clinical disease severity up to 4 years later (Table 3), with larger *BrainAGE* scores being related to worse cogni-

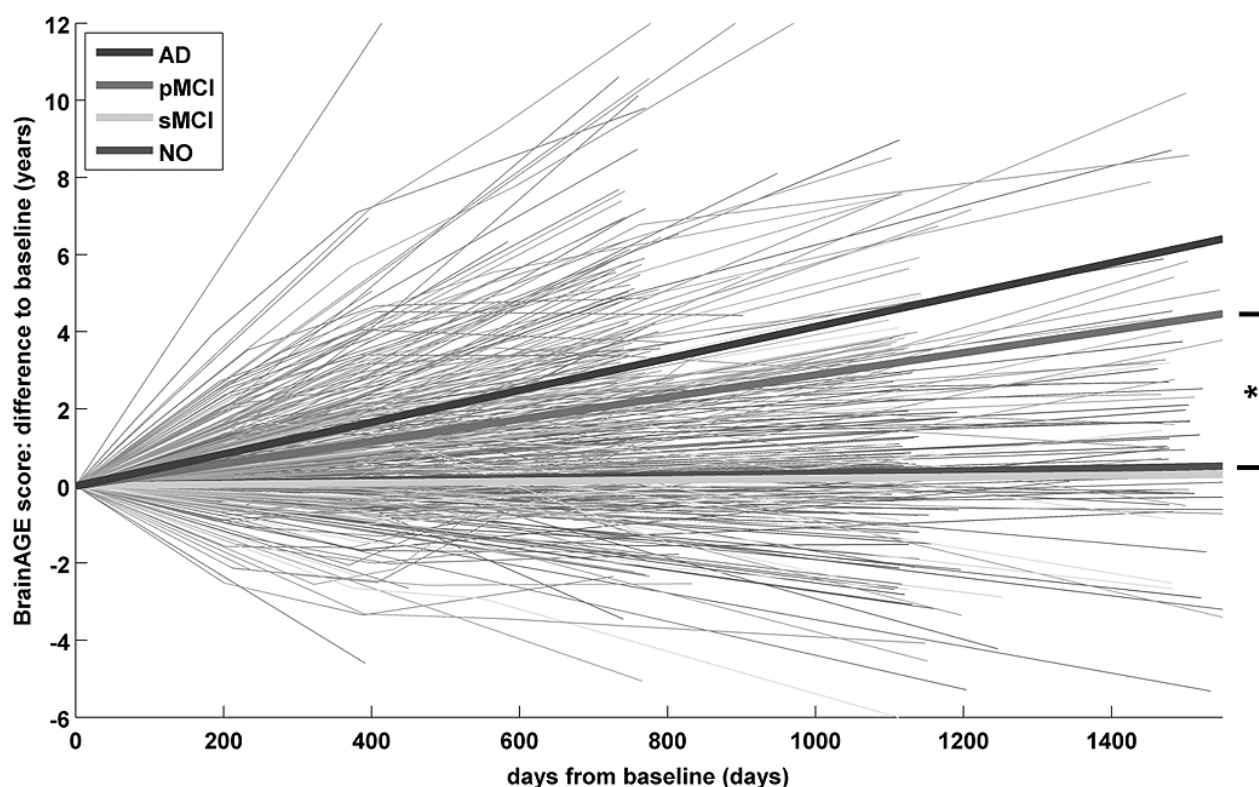


Figure 5. Longitudinal changes in *BrainAGE* scores for NO (purple), sMCI (green), pMCI (red), and AD (blue). Thin lines represent individual changes in *BrainAGE* over time; thick lines indicate estimated average changes for each group. Posthoc *t*-tests showed significant differences in the longitudinal *BrainAGE* changes between NO/sMCI vs. pMCI/AD ($p < .05$; black lines).

Table 3. Correlation coefficients between *BrainAGE* and cognitive functioning (ADAS scores) as well as disease severity (MMSE & CDR scores) for the whole test sample as well as for each diagnostic group separately

		NO	sMCI	pMCI	AD	Whole sample
Correlation with baseline <i>BrainAGE</i> score	MMSE score at last scan	-0.14	0.09	-0.18	-0.38***	-0.46***
	CDR score at last scan	-0.04	0.03	0.13	0.24**	0.39***
	ADAS score at last scan	-0.03	-0.24	0.33***	0.31***	0.45***
Correlation with <i>BrainAGE</i> score at last scan	MMSE score at last scan	-0.12	0.01	-0.28**	-0.46***	-0.55***
	CDR score at last scan	0.01	-0.09	0.20*	0.30***	0.46***
	ADAS score at last scan	-0.04	-0.10	0.40***	0.37***	0.55***
Correlation with change in <i>BrainAGE</i> score (baseline – last scan)	MMSE change	0.09	-0.29	-0.23*	-0.23**	-0.33***
	CDR change	0.13	-0.27	0.19*	0.19*	0.27***
	ADAS change	-0.10	-0.04	0.29**	0.16*	0.30***

* $p < .05$, ** $p < .01$, *** $p < .001$. Please explain use of bold and italics!

tive functioning and more severe clinical symptoms ($r = 0.39$ – 0.46). The *BrainAGE* scores based on the last MRI scan correlated even slightly stronger with cognitive scores and clinical severity of the last follow-up visit ($r = 0.46$ – 0.55). The changes in *BrainAGE* scores were also related to the individual changes in all of the three scores ($r = 0.27$ – 0.33). These results denote a close relationship between accelerated brain aging and prospective worsening

of cognitive functioning within the whole sample, i.e., within the full variance of cognitive as well as *BrainAGE* scores.

Even more interesting, when analyzing each diagnostic group separately, we found these relationships between *BrainAGE* and cognitive as well as severity scores were only in the pMCI and AD groups, but not in sMCI and NO groups (Table 3). In pMCI, the strongest correlation with

BrainAGE was found in ADAS ($r = 0.40$; $p < .001$), which is a rather cognitive scale. In AD, the strongest correlation with *BrainAGE* was found in MMSE ($r = -0.46$; $p < .001$), which is commonly used to measure disease severity in AD. These results strongly support the recent result of profound accelerated brain aging being related to disease severity, most pronounced in subjects being already diagnosed with AD, and prospective worsening of cognitive functioning, most pronounced in pMCI subjects.

Discussion

This study described and implemented a novel MRI-based biomarker, aggregating the complex, multidimensional aging pattern across the whole brain into one single value, i.e., the *BrainAGE* score that directly quantifies acceleration or deceleration in individual brain aging. The *BrainAGE* framework comprises well-established and fully automated processing of the T1-weighted MR images and allows one to combine data from different MRI scanners. With correlations between chronological age and estimated brain age of $r = 0.92$ in healthy adults, aged 20–86 years (Franke et al., 2010), and $r = 0.93$ in healthy children and adolescents, aged 5–18 years (Franke et al., 2012), the *BrainAGE* framework has proved to be a straightforward method of accurately and reliably estimating brain age with minimal preprocessing and parameter optimization. Most remarkably, although brain maturation in childhood as well as brain aging in late life comprise very complex, multidimensional, and highly variable processes (Good et al., 2001; Lebel & Beaulieu, 2011; Lenroot & Giedd, 2006; Wilke, Schmithorst, & Holland, 2003), the confidence intervals of estimated brain age did not change as a function of age (Franke et al., 2012, 2010). This underlines the great potential of the approach to correctly capture the multidimensional characteristics of the different maturational and aging processes occurring in childhood and old age, respectively.

Here, the *BrainAGE* framework was trained with whole-brain structural MRI data of about 560 healthy subjects, aged 20–86 years. The model of healthy brain aging was then applied to new data samples. First, the stability of individual *BrainAGE* scores was examined. With ICCs 0.93 and 0.90 between the *BrainAGE* scores calculated from two shortly delayed scans on the same MRI scanner and on different 1.5T and 3.0T scanners, respectively, the *BrainAGE* framework proved its ability to provide reliable estimates.

The sample-specific offsets that emerged in the estimation of *BrainAGE* scores seem to depend on the kind of MRI scanner used, its field-strength, the scanning sequences, and other sample-specific parameters. Therefore, the influences of varying image quality and segmentation quality in training and test data on brain-age estimation quality limit the reliability of the proposed method and should thus be

carefully controlled in future studies as well as analyzed further within even larger samples. But since these offsets proved to be systematic in all subjects within the same sample, it can be easily controlled for by a linear shift. When quantifying brain aging and comparing *BrainAGE* in different clinical samples, one should include samples of healthy subjects in order to control for potential sample- and/or MRI scanner-specific offsets in the estimated scores. There is no need to include control subjects to correct for potential offsets when examining only the relation between *BrainAGE* and other measures or the difference between brain aging in two subsamples of the same sample. Here, the *BrainAGE* framework is robust and can furthermore be applied to and generalized across different scanners. These results are in line with Klöppel et al. (2008), indicating that the effect of the scanner is sufficiently different from that of aging processes.

Regarding the relevance within the clinical context, the *BrainAGE* approach again proved its potential to indicate accelerated brain aging based on structural MRI data. Subjects with AD and subjects with MCI who converted to AD and cognitively declined within 3 years of follow-up (pMCI) exhibited significantly larger baseline *BrainAGE* scores compared to control subjects and those with MCI who remained cognitively stable (sMCI). Further, the *BrainAGE* framework even proved its capability of recognizing accelerated brain atrophy in a longitudinal design. Already starting with a higher baseline *BrainAGE* score of about 6 to 7 years in pMCI and AD, brain aging accelerates even more during follow-up, at the speed of 1 additional year in brain atrophy per follow-up year in pMCI subjects and 1.5 additional years in brain atrophy per follow-up year in AD patients. This accumulated to a mean *BrainAGE* score of about 9 years at the last scan in both groups, with mean follow-up durations of 2.6 years for pMCI and 1.7 years for AD. Compared to that, sMCI and healthy control subjects did not show any deviations from healthy brain aging at baseline or at follow-up. These results are in line with recent studies that showed increased GM atrophy of approximately 2% per year in AD (Anderson et al., 2012), accelerated changes in whole brain volume in MCI (Driscoll et al., 2009), acceleration in atrophy rates as subjects progress from MCI to AD (Jack et al., 2008), and greater GM loss in certain regions in pMCI subjects (Chetelat et al., 2005; Desikan et al., 2008; Leow et al., 2009; McDonald et al., 2012; Sluimer et al., 2009). Furthermore, our results also support the assumption of AD being a form of or at least being associated with accelerated aging (Cao et al., 2010; Driscoll et al., 2009; Dukart et al., 2011; Jones et al., 2011; Saetre et al., 2011; Spulber et al., 2010).

Additionally, the individual *BrainAGE* scores were clearly related to measures of severity of clinical disease, most pronounced in subjects already diagnosed as AD, as well as cognitive functioning, most pronounced in MCI subjects converting to AD within the next 3 years. Even more interestingly and clinically valuable, the *BrainAGE* scores estimated at baseline were already moderately cor-

related to the prospective worsening of cognitive functioning within the next 3 years. Cognitive decline was recently found to progressively accelerate years before being diagnosed as AD (Wilson, Leurgans, Boyle, & Bennett, 2011), and be correlated with the atrophy rates in specified brain regions (Desikan et al., 2008). Our results support the suggested relationship between progressive acceleration in brain aging and rate of change in cognitive functioning as well as clinical severity in pMCI and AD during follow-up. Furthermore, we could even show a distinct pattern of accelerated brain aging in pMCI subjects being more closely related to the worsening of higher cognitive functions, but slightly less with disease severity, whereas in AD patients accelerated brain aging was more closely related to disease severity and slightly less with the worsening of higher cognitive functions. Regarding NO and sMCI subjects, a ceiling effect was observed as well as a slightly lower variance within the cognitive scores. This may be mainly due to the fact that the scales analyzed in this study were used specifically to identify clinical disease severity as well as deterioration in cognitive functioning in the ADNI sample. Future work should further explore the relationship between *BrainAGE* and cognitive functioning with cognitive scales that are more appropriate to capture healthy cognitive aging.

In conclusion, the *BrainAGE* framework demonstrated its potential to reliably indicate accelerated brain aging. Since an additional increase in *BrainAGE* scores as well as profound relationships to disease severity and prospective worsening of cognitive functions were found in pMCI and AD during follow-up, the validity of individual *BrainAGE* scores indicating accelerated brain aging is further strengthened. Future work should demonstrate the applicability of the *BrainAGE* method on a single subject level in order to indicate early on those people at risk for converting to AD. Recently, we already demonstrated the capability of the *BrainAGE* approach to work on a single subject level by classifying subjects as either children (age range 5–10 years) or adolescents (age range 13–18 years), based on their estimated brain age, with 97% accuracy (sensitivity = 98%, specificity = 96%; Franke et al., 2012).

The implication of these results is that this approach could potentially lead to improved identification of people at risk of faster degradation of brain structure and function and potential risk for AD, thus contributing to an early diagnosis of neurodegenerative diseases, and facilitate early treatment or a preventative intervention. Depending on the availability of subject data, future explorations could include applying this approach to several risk factors for accelerated brain aging and dementia, like diabetes (de Bresser et al., 2010; van Elderen et al., 2010), the metabolic syndrome (Solfrizzi et al., 2011), or other lifestyle factors (Chen, Lin, & Chen, 2009; Clarke, 2006; Scarmeas et al., 2009; Solfrizzi et al., 2008), to predict the severity of clinical symptoms or the rate of cognitive decline, to differentiate between different kinds of dementia (e.g., fronto-temporal dementia), and to evaluate the therapeutic effect of

drugs or other treatment modalities. Additionally, since individual quality of life is increasingly being suggested as a crucial outcome variable for health-improving and preventive interventions in old age (Garratt, Schmidt, Mackintosh, & Fitzpatrick, 2002; Martin, Schneider, Eicher, & Moor, 2012), it may be enlightening to integrate the *BrainAGE* approach into the recently presented “functional quality of life” (*fQOL*) model (Martin et al., 2012). This model determines the quality of life with a dynamic approach, allowing the testing of the complex relations between individual functionality judgments (e.g., individual resources, activities, central life domains) and how these relations can be adapted to stabilize or increase individual *fQOL*. Moreover, the *fQOL* can be applied to compare between and within subjects across the lifespan. Hence, future work may examine the functional value of individual *BrainAGE* scores and its complex interactions with *fQOL*-determining variables such as subjective representations as well as evaluations of cognitive performance (e.g., memory) in order to finally determine individuals’ overall quality of life.

Consequently, in the future this novel *BrainAGE* approach may prove clinically valuable in detecting both normal and abnormal brain aging, providing important prognostic information.

Acknowledgments

We are grateful to Alissa Winkler, PhD, for her comments on the manuscript. This work was supported in part by BMBF grants 01EV0709 and 01GW0740.

Data collection and sharing for this project was funded by the Alzheimer’s Disease Neuroimaging Initiative (ADNI, National Institutes of Health Grant U01 AG024904; <http://adni.loni.ucla.edu>). ADNI is funded by the National Institute on Aging, the National Institute of Biomedical Imaging and Bioengineering, and through generous contributions from the following organizations (also available at http://adni.loni.ucla.edu/wp-content/uploads/how_to_apply/ADNI_Acknowledgment_List.pdf): Abbott; Alzheimer’s Association; Alzheimer’s Drug Discovery Foundation; Amorfix Life Sciences Ltd.; AstraZeneca; Bayer HealthCare; BioClinica, Inc.; Biogen Idec Inc.; Bristol-Myers Squibb Company; Eisai Inc.; Elan Pharmaceuticals Inc.; Eli Lilly and Company; F. Hoffmann-La Roche Ltd. and its affiliated company Genentech, Inc.; GE Healthcare; Innogenetics, N. V.; IXICO Ltd.; Janssen Alzheimer Immunotherapy Research & Development, LLC.; Johnson & Johnson Pharmaceutical Research & Development LLC.; Medpace, Inc.; Merck & Co., Inc.; Meso Scale Diagnostics, LLC.; Novartis Pharmaceuticals Corporation; Pfizer Inc.; Servier; Synarc Inc.; and Takeda Pharmaceutical Company. The Canadian Institutes of Health Research provides funds to support ADNI clinical sites in Canada. Private sector contributions are facilitated by the Foundation for the National Institutes of Health (www.fnih.org). The grantee organization is the Northern

California Institute for Research and Education, and the study is coordinated by the Alzheimer's Disease Cooperative Study at the University of California, San Diego. ADNI data are disseminated by the Laboratory for Neuro Imaging at the University of California, Los Angeles. This research was also supported by NIH grants P30 AG010129 and K01 AG030514.

References

[Complete journal names, please]

- Anderson, V.M., Schott, J.M., Bartlett, J.W., Leung, K.K., Miller, D.H., & Fox, N.C. (2012). Gray matter atrophy rate as a marker of disease progression in AD. *Neurobiol Aging*, *33*, 1194–1202.
- Ashburner, J., Csernansky, J.G., Davatzikos, C., Fox, N.C., Frisone, G.B., & Thompson, P.M. (2003). Computer-assisted imaging to assess brain structure in healthy and diseased brains. *Lancet Neurology*, *2*(2), 79–88.
- Ashburner, J., & Friston, K.J. (2005). Unified segmentation. *Neuroimage*, *26*, 839–851.
- Bishop, C.M. (2006). *Pattern recognition and machine learning*. New York, NY: Springer.
- Cao, K., Chen-Plotkin, A.S., Plotkin, J.B., & Wang, L.S. (2010). Age-correlated gene expression in normal and neurodegenerative human brain tissues. *PLoS One*, *5*(9) [PAGE NOS?].
- Chen, J.H., Lin, K.P., & Chen, Y.C. (2009). Risk factors for dementia. *J Forms Med Assoc*, *108*, 754–764.
- Chetelat, G., Landeau, B., Eustache, F., Mezenge, F., Viader, F., de la Sayette, V., . . . Baron, J.C. (2005). Using voxel-based morphometry to map the structural changes associated with rapid conversion in MCI: A longitudinal MRI study. *Neuroimage*, *27*, 934–946.
- Clarke, R. (2006). Vitamin B12, folic acid, and the prevention of dementia. *New England Journal of Medicine*, *354*, 2817–2819.
- Cockrell, J.R., & Folstein, M.F. (1988). Mini-Mental State Examination (MMSE). *Psychopharmacol Bull*, *24*, 689–692.
- Cuadra, M.B., Cammoun, L., Butz, T., Cuisenaire, O., & Thiran, J.P. (2005). Comparison and validation of tissue modelization and statistical classification methods in T1-weighted MR brain images. *IEEE Trans Med Imaging*, *24*, 1548–1565.
- de Bresser, J., Tiehuis, A.M., van den Berg, E., Reijmer, Y.D., Jongen, C., Kappelle, L.J., . . . Biessels, G.J. (2010). Progression of cerebral atrophy and white matter hyperintensities in patients with type 2 diabetes. *Diabetes Care*, *33*, 1309–1314.
- Desikan, R.S., Fischl, B., Cabral, H.J., Kemper, T.L., Guttman, C.R., Blacker, D., . . . Killiany, R.J. (2008). MRI measures of temporoparietal regions show differential rates of atrophy during prodromal AD. *Neurology*, *71*, 819–825.
- Driscoll, I., Davatzikos, C., An, Y., Wu, X., Shen, D., Kraut, M., & Resnick, S.M. (2009). Longitudinal pattern of regional brain volume change differentiates normal aging from MCI. *Neurology*, *72*, 1906–1913.
- Dukart, J., Schroeter, M.L., & Mueller, K. (2011). Age correction in dementia – matching to a healthy brain. *PLoS One*, *6*(7), e22193.
- Franke, K., Luders, E., May, A., Wilke, M., & Gaser, C. (2012). Brain maturation: Predicting individual *BrainAGE* in children and adolescents using structural MRI. *NeuroImage*. <http://dx.doi.org/10.1016/j.neuroimage.2012.08.001>.
- Franke, K., Ziegler, G., Klöppel, S., Gaser, C., & Initiative, A.S.D.N. (2010). Estimating the age of healthy subjects from T1-weighted MRI scans using kernel methods: exploring the influence of various parameters. *Neuroimage*, *50*, 883–892.
- Garratt, A., Schmidt, L., Mackintosh, A., & Fitzpatrick, R. (2002). Quality of life measurement: bibliographic study of patient assessed health outcome measures. *British Medical Journal*, *324*, 1417.
- Gaser, C. (2009). Partial volume segmentation with Adaptive Maximum a Posteriori (MAP) approach. *NeuroImage*, *47*, S121.
- Gogtay, N., & Thompson, P.M. (2010). Mapping gray matter development: Implications for typical development and vulnerability to psychopathology. *Brain Cogn*, *72*(1), 6–15.
- Good, C.D., Johnsrude, I.S., Ashburner, J., Henson, R.N., Friston, K.J., & Frackowiak, R.S. (2001). A voxel-based morphometric study of aging in 465 normal adult human brains. *Neuroimage*, *14*(1 Pt 1), 21–36.
- Jack, C.R., Jr., Weigand, S.D., Shiung, M.M., Przybelski, S.A., O'Brien, P.C., Gunter, J.L., . . . Petersen, R.C. (2008). Atrophy rates accelerate in amnesic mild cognitive impairment. *Neurology*, *70*(19 Pt 2), 1740–1752.
- Jones, D.T., Machulda, M.M., Vemuri, P., McDade, E.M., Zeng, G., Senjem, M.L., . . . Jack, C.R., Jr. (2011). Age-related changes in the default mode network are more advanced in Alzheimer disease. *Neurology*, *77*, 1524–1531.
- Klöppel, S., Stonnington, C.M., Chu, C., Draganski, B., Scahill, R.I., Rohrer, J.D., . . . Frackowiak, R.S.J. (2008). Automatic classification of MR scans in Alzheimer's disease. *Brain*, *131*(Pt 3), 681–689.
- Lebel, C., & Beaulieu, C. (2011). Longitudinal development of human brain wiring continues from childhood into adulthood. *J Neurosci*, *31*, 10937–10947.
- Lenroot, R.K., & Giedd, J.N. (2006). Brain development in children and adolescents: Insights from anatomical magnetic resonance imaging. *Neurosci Biobehav Rev*, *30*, 718–729.
- Leow, A.D., Yanovsky, I., Parikshak, N., Hua, X., Lee, S., Toga, A.W., . . . Thompson, P.M. (2009). Alzheimer's disease neuroimaging initiative: A one-year follow-up study using tensor-based morphometry correlating degenerative rates, biomarkers and cognition. *Neuroimage*, *45*, 645–655.
- Marcus, D.S., Wang, T.H., Parker, J., Csernansky, J.G., Morris, J.C., & Buckner, R.L. (2007). Open Access Series of Imaging Studies (OASIS): Cross-sectional MRI data in young, middle-aged, nondemented, and demented older adults. *J Cogn Neurosci*, *19*, 1498–1507.
- Martin, M., Schneider, R., Eicher, S., & Moor, C. (2012). The Functional Quality of Life (fQOL)-model. A new basis for quality of life-enhancing interventions in old age. *GeroPsych*, *25*, 33–40.
- McDonald, C.R., Gharapetian, L., McEvoy, L.K., Fennema-Notestine, C., Hagler, D.J., Jr., Holland, D., & Dale, A.M. (2012). Relationship between regional atrophy rates and cognitive decline in mild cognitive impairment. *Neurobiol Aging*, *33*, 242–253.
- Meda, S.A., Giuliani, N.R., Calhoun, V.D., Jagannathan, K., Schretlen, D.J., Pulver, A., . . . Pearlson, G.D. (2008). A large scale ($N = 400$) investigation of gray matter differences in

- schizophrenia using optimized voxel-based morphometry. *Schizophrenia Research*, 101(1–3), 95–105.
- Mohs, R. C. (1996). The Alzheimer's Disease Assessment Scale. *Int Psychogeriatr*, 8, 195–203.
- Mohs, R. C., & Cohen, L. (1988). Alzheimer's Disease Assessment Scale (ADAS). *Psychopharmacol Bull*, 24, 627–628.
- Morris, J. C. (1993). The Clinical Dementia Rating (CDR): Current version and scoring rules. *Neurology*, 43, 2412–2414.
- Pfefferbaum, A., Mathalon, D. H., Sullivan, E. V., Rawles, J. M., Zipursky, R. B., & Lim, K. O. (1994). A quantitative magnetic resonance imaging study of changes in brain morphology from infancy to late adulthood. *Arch Neurol*, 51, 874–887.
- Rajapakse, J. C., Giedd, J. N., & Rapoport, J. L. (1997). Statistical approach to segmentation of single-channel cerebral MR images. *IEEE Trans Med Imaging*, 16, 176–186.
- Saetre, P., Jazin, E., & Emilsson, L. (2011). Age-related changes in gene expression are accelerated in Alzheimer's disease. *Synapse*, 65, 971–974.
- Scarmeas, N., Luchsinger, J. A., Schupf, N., Brickman, A. M., Cosentino, S., Tang, M. X., & Stern, Y. (2009). Physical activity, diet, and risk of Alzheimer disease. *Journal of the American Medical Association*, 302, 627–637.
- Schölkopf, B., & Smola, A. (2002). *Learning with Kernels: Support vector machines, regularization, optimization, and beyond*. Cambridge, MA: MIT.
- Silk, T. J., & Wood, A. G. (2011). Lessons about neurodevelopment from anatomical magnetic resonance imaging. *J Dev Behav Pediatr*, 32, 158–168.
- Sluimer, J. D., van der Flier, W. M., Karas, G. B., van Schijndel, R., Barnes, J., Boyes, R. G., . . . Barkhof, F. (2009). Accelerating regional atrophy rates in the progression from normal aging to Alzheimer's disease. *Eur Radiol*, 19, 2826–2833.
- Solfrizzi, V., Capurso, C., D'Introno, A., Colacicco, A. M., Santamato, A., Ranieri, M., . . . Panza, F. (2008). Lifestyle-related factors in predementia and dementia syndromes. *Expert Rev Neurother*, 8(1), 133–158.
- Solfrizzi, V., Scafato, E., Capurso, C., D'Introno, A., Colacicco, A. M., Frisardi, V., . . . Panza, F. (2011). Metabolic syndrome, mild cognitive impairment, and progression to dementia. *The Italian Longitudinal Study on Aging. Neurobiol Aging*, 32, 1932–1941.
- Spulber, G., Niskanen, E., MacDonald, S., Smilovici, O., Chen, K., Reiman, E. M., . . . Soininen, H. (2010). Whole brain atrophy rate predicts progression from MCI to Alzheimer's disease. *Neurobiol Aging*, 31, 1601–1605.
- Terribilli, D., Schaufelberger, M. S., Duran, F. L. S., Zanetti, M. V., Curiati, P. K., Menezes, P. R., . . . Busatto, G. F. (2009). Age-related gray matter volume changes in the brain during nonelderly adulthood. *Neurobiology of Aging*. doi 10.1016/j.neurobiolaging.2009.1002.1008
- Tipping, M. (2000). The relevance vector machine. In S. A. Solla, T. K. Leen, & K.-R. Müller (Eds.), *Advances in neural information processing systems 12* (pp. 652–658). [city?]: MIT.
- Tipping, M. E. (2001). Sparse bayesian learning and the relevance vector machine. *Journal of Machine Learning Research*, 1, 211–244.
- Toga, A. W., Thompson, P. M., & Sowell, E. R. (2006). Mapping brain maturation. *Trends in Neurosciences*, 29, 148–159.
- Tohka, J., Zijdenbos, A., & Evans, A. (2004). Fast and robust parameter estimation for statistical partial volume models in brain MRI. *Neuroimage*, 23, 84–97.
- van Elderen, S. G., de Roos, A., de Craen, A. J., Westendorp, R. G., Blauw, G. J., Jukema, J. W., . . . van der Grond, J. (2010). Progression of brain atrophy and cognitive decline in diabetes mellitus: a 3-year follow-up. *Neurology*, 75, 997–1002.
- Wilke, M., Schmithorst, V. J., & Holland, S. K. (2003). Normative pediatric brain data for spatial normalization and segmentation differs from standard adult data. *Magn Reson Med*, 50, 749–757.
- Wilson, R. S., Leurgans, S. E., Boyle, P. A., & Bennett, D. A. (2011). Cognitive decline in prodromal Alzheimer disease and mild cognitive impairment. *Arch Neurol*, 68, 351–356.

Manuscript submitted: 29.6.2012

Manuscript accepted after revision: 11.9.2012

Katja Franke

Structural Brain Mapping Group
 Department of Psychiatry
 University of Jena
 Jahnstr. 3
 DE-07743 Jena
 Germany
 Tel. +49 3641-934751
 Fax +49 3641-934755
 katja.franke@uni-jena.de